Appendix G

HYDRODYNAMIC MODELLING REPORT

1 Introduction

This document reports on hydrodynamic modelling undertaken to evaluate dispersion of the effluent discharged from the Aussie Prawns aquaculture development. The effluent is discharged directly into a creek, some 700 m long, that flows into the Middle arm of the Darwin harbour, as shown in Figure 1.1.

A preliminary analysis identified due to the large discharge volumes involved, only limited dispersion is expected to occur within the discharge creek. Accordingly it was decided to concentrate on dispersion of the effluent once it reaches the main water body of the Middle Arm.

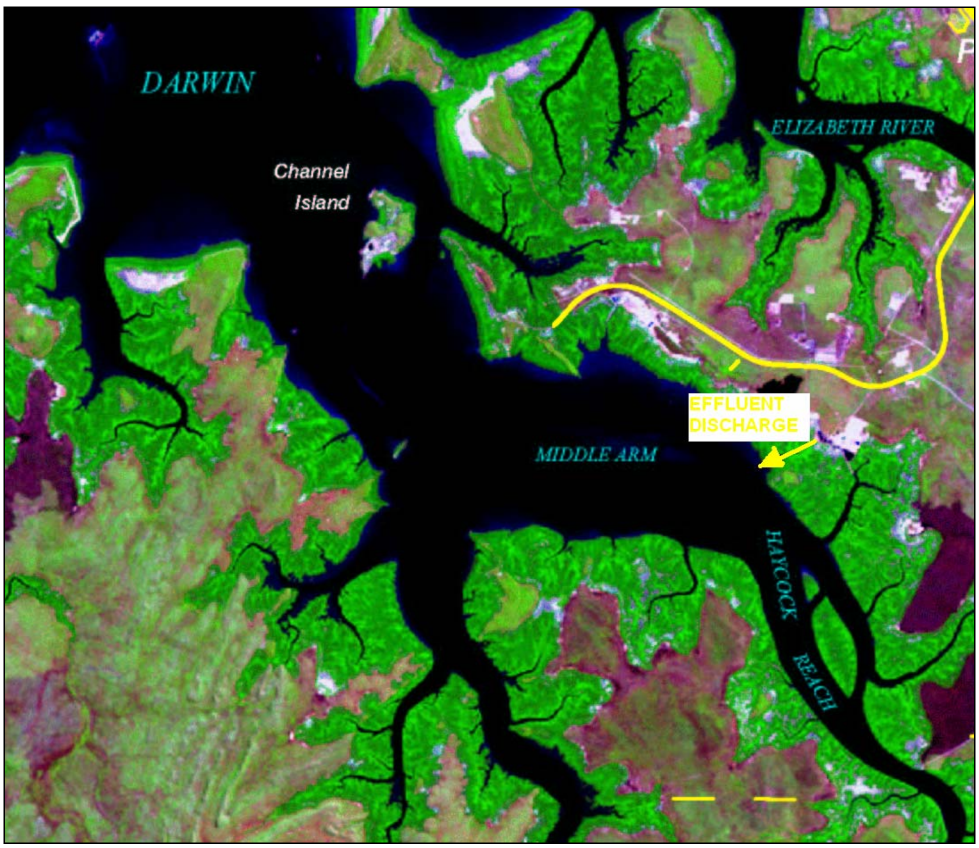

Figure 1.1 Section of Darwin harbour with location of effluent inflow into the Middle Arm

The modelling was undertaken using the three dimensional (3D) oceanographic model previously used successfully by KBR in similar studies. No site specific oceanographic data were available to verify the model in this study the previous numerous applications of the model confirmed that once the correct local bathymetric data are used, in conjunction with governing forces (tide, wind, inflows, etc) the model can predict very accurately the local hydrodynamic processes, i.e. ocean currents and dispersion. However model findings on tidal exchange rates within the Middle Arm are in general agreement with previous work (Wilson et al., 2004).

Local bathymetry was kindly provided by the NT Government modelling team already undertaking hydrodynamic modelling of the same part of the Darwin Harbour (David Williams, 2005).

Review of regional data identified that tides are the main forcing mechanism. Furthermore, it was identified that during the long periods without rainfall in the area, flows from Pioneer Creek and Blackmore River into the Middle Arm are negligible. Accordingly river inflows were conservatively set to zero, while tidal forcing was set as the only forcing mechanism.

The oceanographic model was set up in barotropic mode, i.e. no density effects were included in the present analysis.

A full water quality analysis was beyond the scope of this study. Accordingly, instead of analysing any particular water quality variable, the hydrodynamic model was set up to illustrate dispersion of a conservative tracer by the tidal currents. Any water quality variable that might be of particular interest would experience a similar dispersion pattern but it would also experience changes (most likely reduction) in concentration as a result of biological processes. Therefore, the methodology employing a conservative tracer (i.e. "dye") represents a conservative approach, as it is likely to lead to larger spatial extent of the zone of influence of the effluent expected for a particular water quality variable.

2 Model description and input data

The three-dimensional numerical model known as the **Ham**burg **S**helf **O**cean **M**odel (HAMSOM) has been used in this study. The model was originally developed for oceanographic studies in the North Sea (Backhaus and Hainbucher 1986). However, it has been used at a number of locations around the world (Backhaus *et al*. 1987; Pohlmann 1986; Stronach *et al.* 1993).

The model has been successfully applied in the analysis of the hydrodynamic processes during the Perth Coastal Waters Study (Pattiaratchi and Knock 1995) and was used by KBR in the Perth Long-term Ocean Outlet Monitoring programme (Kinhill 1997a, 1997b, 1998a, 1999, KBR 2004).

The same model was used in assessment of the likely environmental impact for several aquaculture developments (Kinhill 2000, KBR 2001 a,b).

Description of the model is provided in Appendix A.

Input data

Data including bathymetry, tidal forcing and expected effluent discharge and characteristics was required for the hydrodynamic modelling.

Details of the computational domains used for hydrodynamic simulations are presented in Figure 2.1. Considering that zero flow was assumed in Pioneer Creek and Blackmore River only their lower reaches were included in the model. Within the close vicinity of the mangrove creek inflow into the main water body, the grid spacing was reduced to 75 m x 75 m. These smaller-sized cells allowed for increased modelling detail in this region. The computational grid away from the mangrove creek inflow into the main water body was coarser. Considering that no flow was assumed from Pioneer Creek and Blackmore Rriver, the computational grid was designed to account only for their lower reaches.

Parameters of interest used in the simulations are provided in Table 2.1.

Table 2.1 - Parameters used in the numerical simulations

Parameter	
Number of cells N–S (horizontal plane)	65
Number of cells E–W (horizontal plane)	80
Number of layers (vertical plane)	4
Typical grid size in horizontal plane (m)	variable
Layer 1 to 4 depths (m)	5, 10, 15, sea floor
Δt time step (sec)	40
F_c bottom friction (-)	2.4×10^{-3}
A_H horizontal eddy viscosity (m^2/s)	20
Boundary conditions at open boundaries	Orlanski

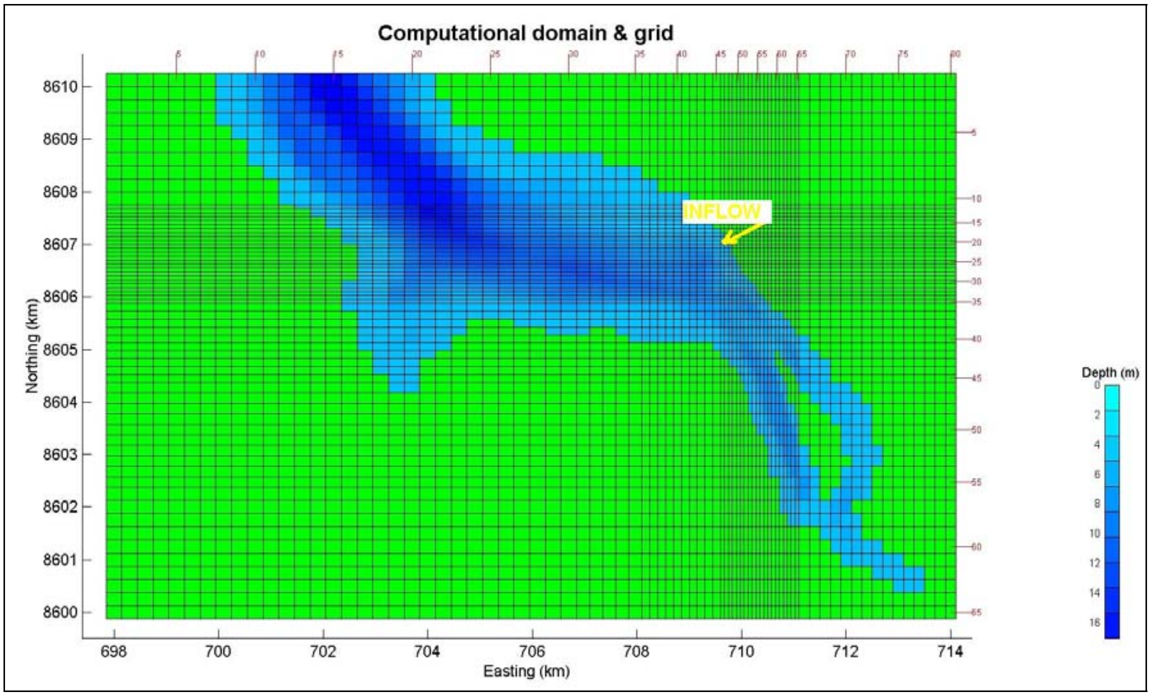

Figure 2.1 - Computational grid showing water depth used for modelling

Modelling was undertaken over a period of about one month. Tidal forcing, applied at the northern boundary of the model over the simulated period, is shown in Figure 2.2.

Typical diurnal effluent discharge pattern for the prawn farm was developed based upon the information from the design team, and shown in Figure 2.3. The timing of discharge was selected to ensure that effluent is discharged at the time when tide recedes, to maximise its flushing effect.

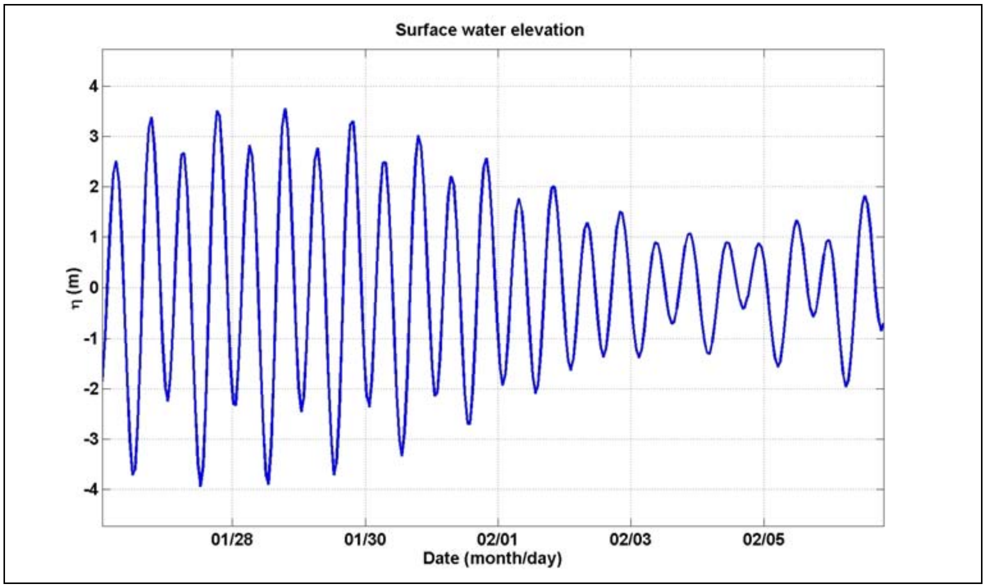

Figure 2.2 – Tidal forcing data used in the analysis

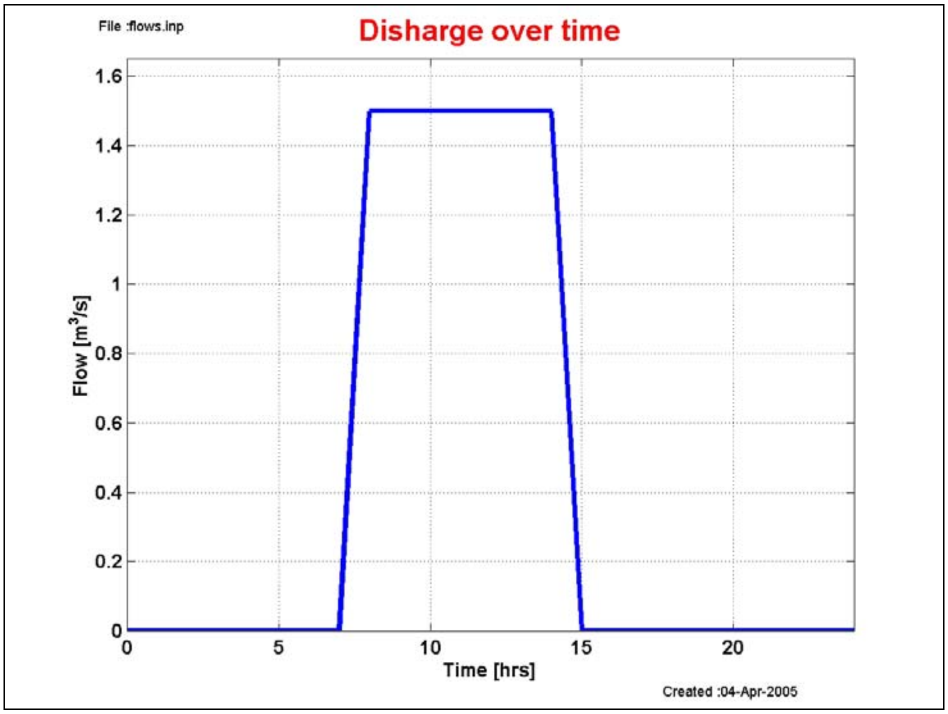

Figure 3.3 – Typical daily discharge pattern from the prawn farm

Figure 3.4 shows concentration of the conservative tracer (i.e. "dye") assumed to be discharged with the flow, shown in relation to the typical daily tidal variations. The initial concentration of the conservative tracer in the receiving water was assumed to be equal to zero.

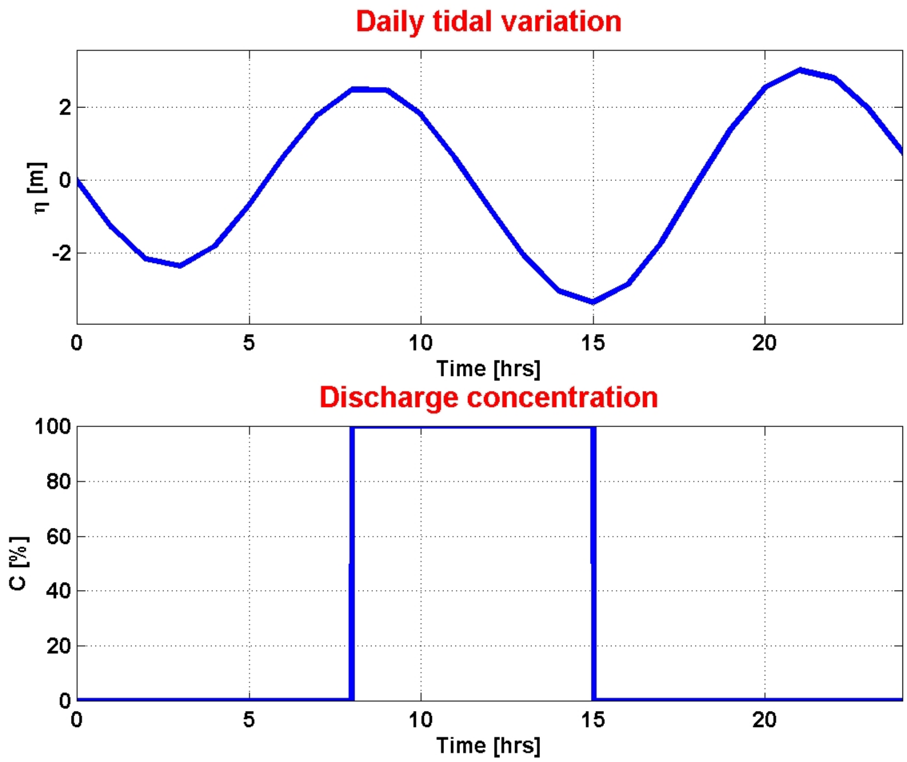

Figure 3.4 – Concentration of conservative tracer in the discharge in relation to typical daily tidal elevations

3 Model results and discussion

Simulations were performed over the period of one month. The tracer was released on Feb 1 at 8:00 AM (see Figure 2.2 for tidal forcing). Results presented below in Figures 3.1 to 3.7 reflect the period before, during and after cessation of discharge, for the first day of operation (Feb 2).

Figure 3.1 shows the concentration of the conservative tracer before the discharge started. Once the discharge starts tracer concentrations, shown in Figure 3.2, increase in the vicinity of the discharge point. The zone with increased concentration is stretched along the shoreline resulting from the strong tidal currents in the area, with the zone with concentration 50% and higher than the ambient conditions encompassing a zone of some 800m in length and some 40 m in width (stretched along the shoreline). Similar patterns can be seen throughout the discharge period, as shown in Figure 3.3 to 3.5. However once the discharge ceases, the concentrations keep falling back to the original conditions.

As discussed in the introduction, these results are expected to provide a good indication of the dispersion patterns of effluent discharge into the Middle arm, while being conservative by assuming fully conservative “dye”. The actual spatial and particularly temporal concentration (i.e. possible build up or lack of it) of a particular water quality variable in the long term would have to take into account biological processes within the Middle creek and the rest of the Darwin Harbour.

Tidally induced flushing provides for the efficient dispersion of the effluent.

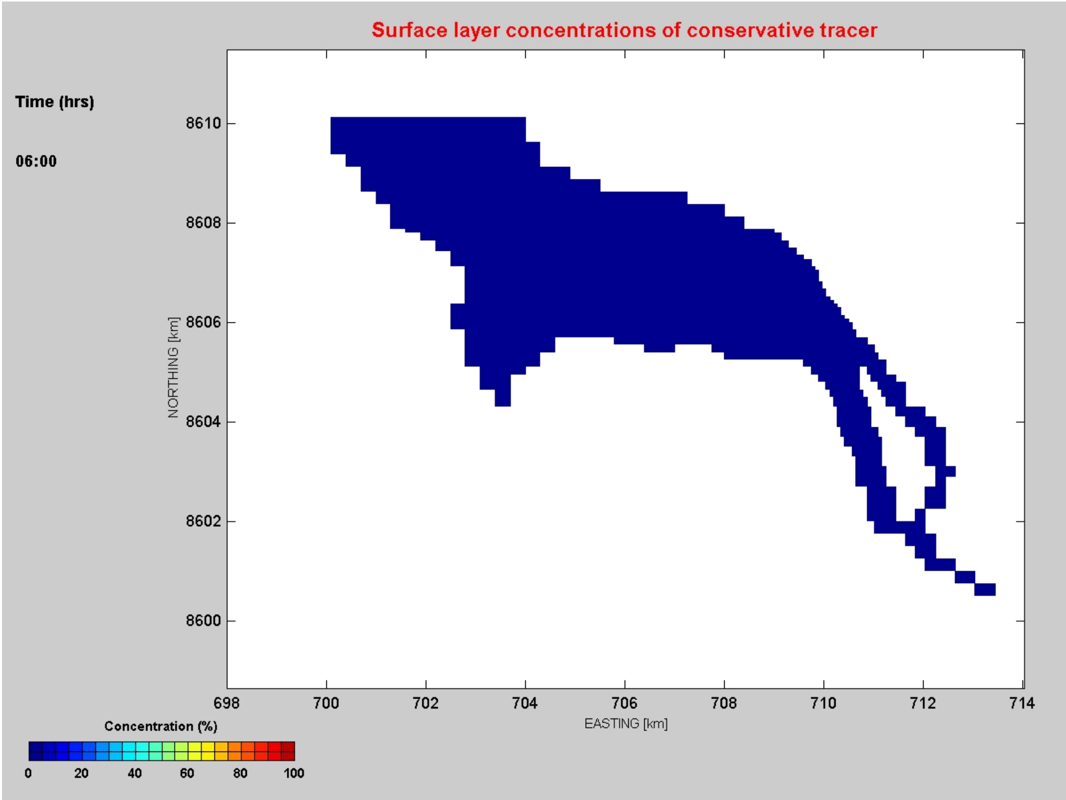

Figure 3.1 – Concentrations of conservative tracer before the start of discharge.

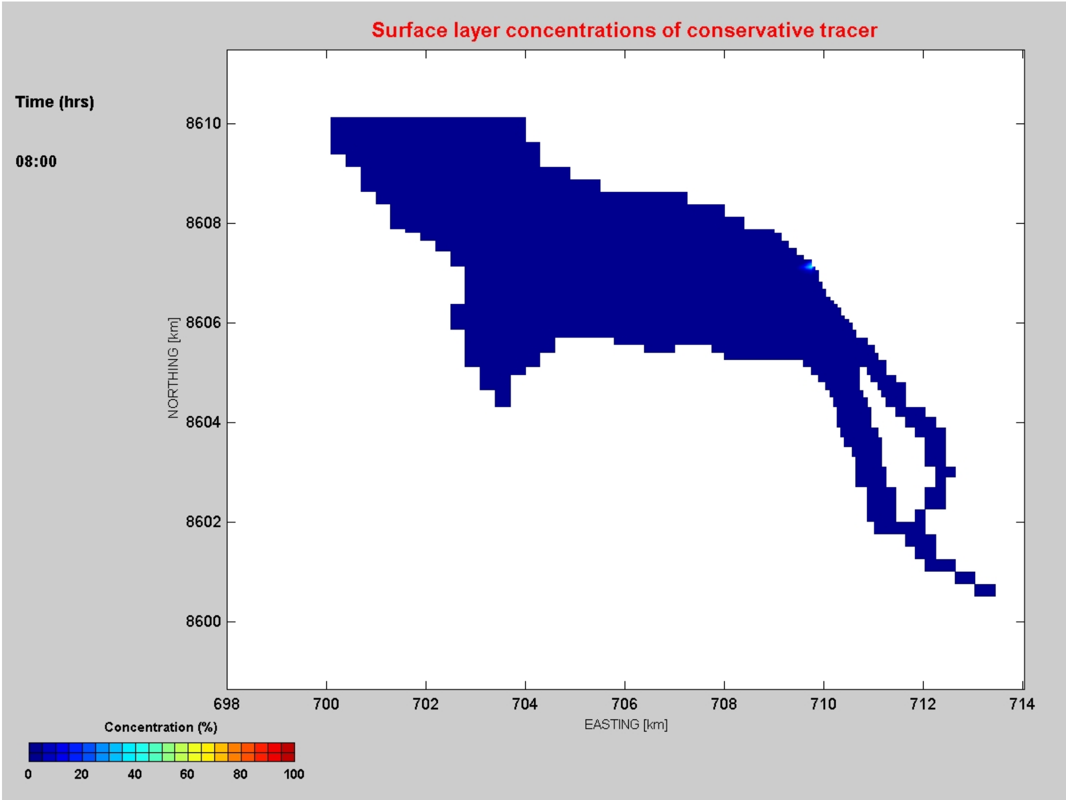

Figure 3.2 – Concentrations of conservative tracer at the start of discharge.

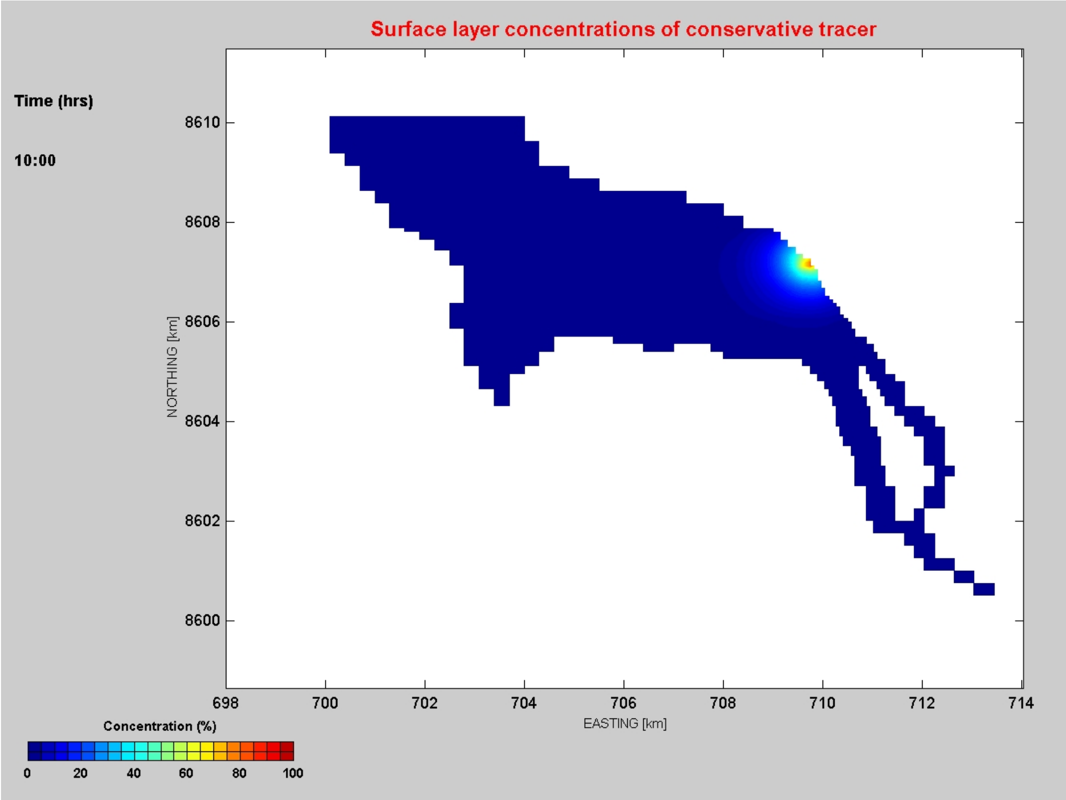

Figure 3.3– Concentrations of conservative tracer after 2 hrs of discharge.

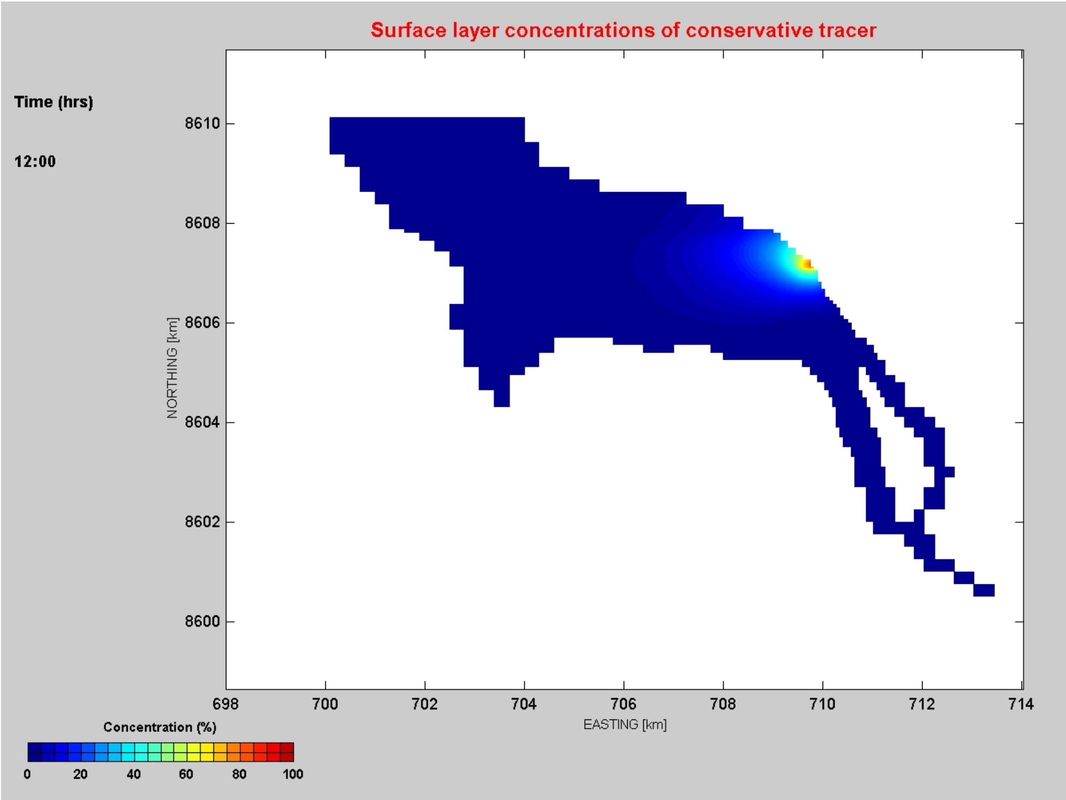

Figure 3.4– Concentrations of conservative tracer after 4 hrs of discharge.

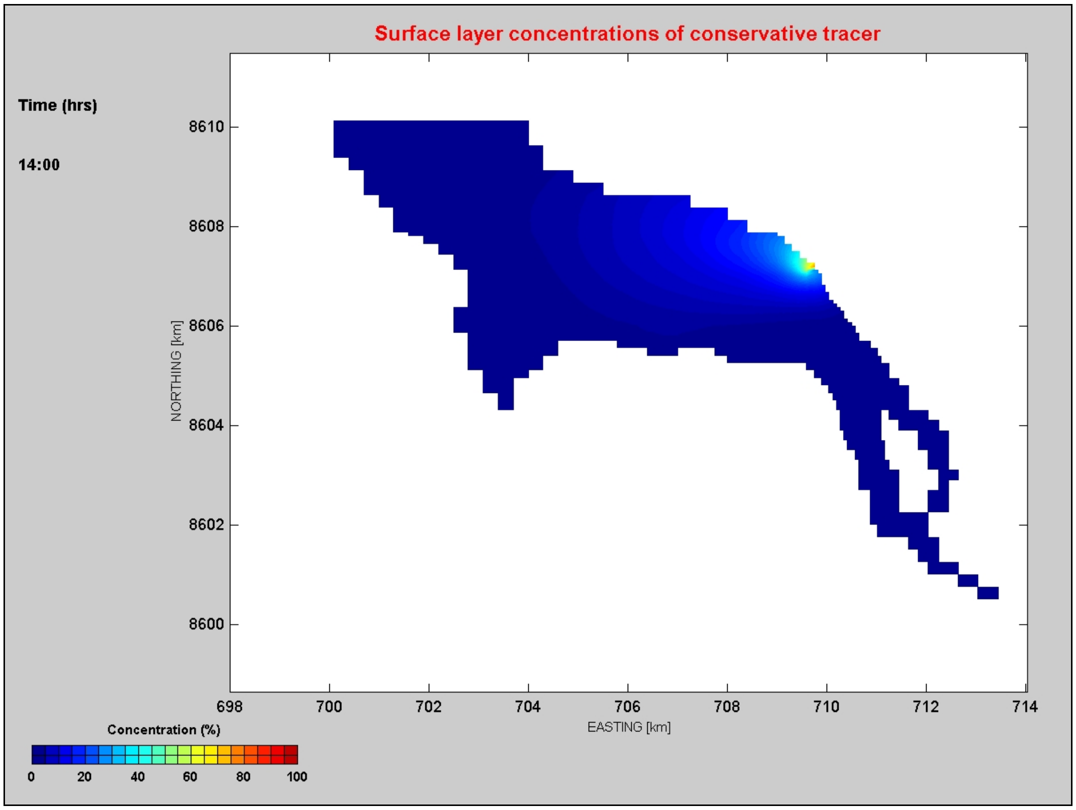

Figure 3.5– Concentrations of conservative tracer after 6 hrs of discharge.

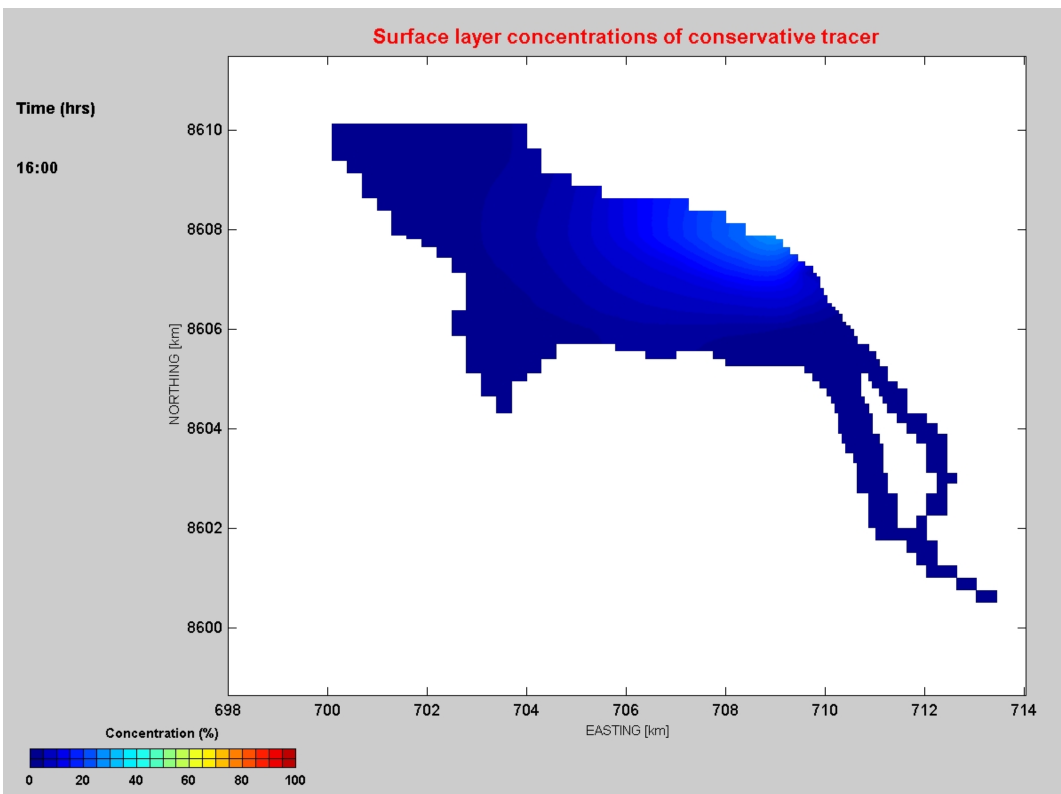

Figure 3.6– Concentrations of conservative tracer after 1 hrs of cease of discharge.

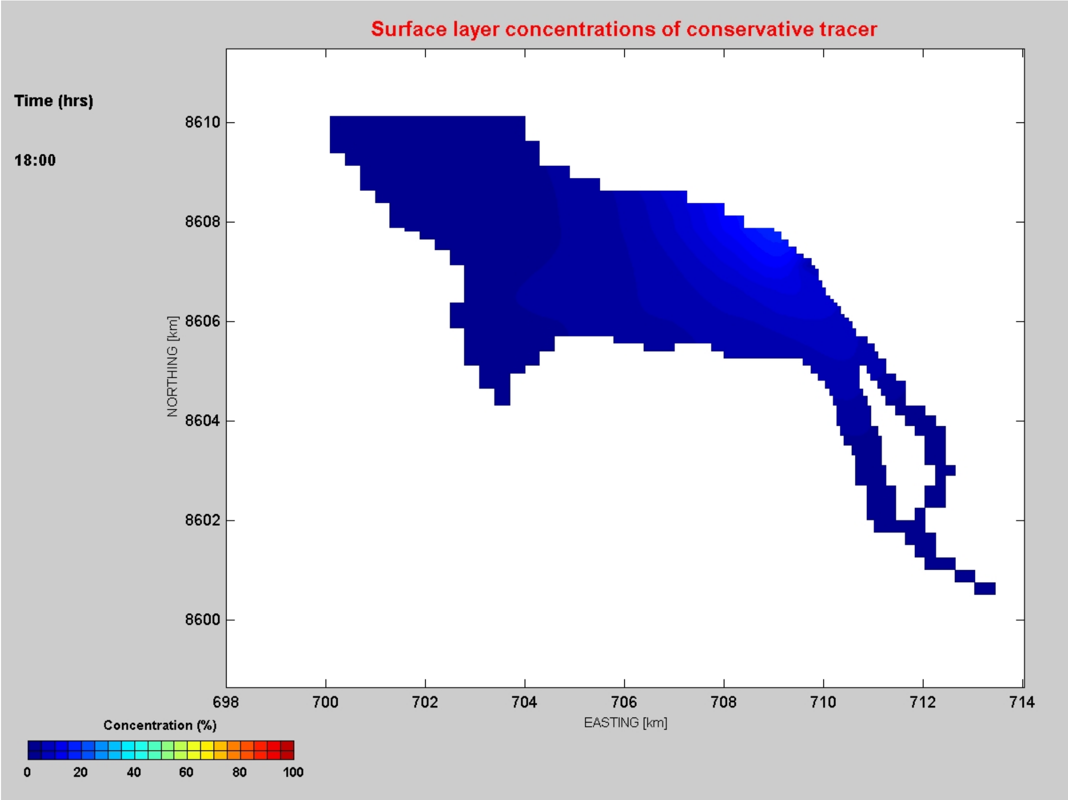

Figure 3.7– Concentrations of conservative tracer after 3 hrs of cease of discharge.

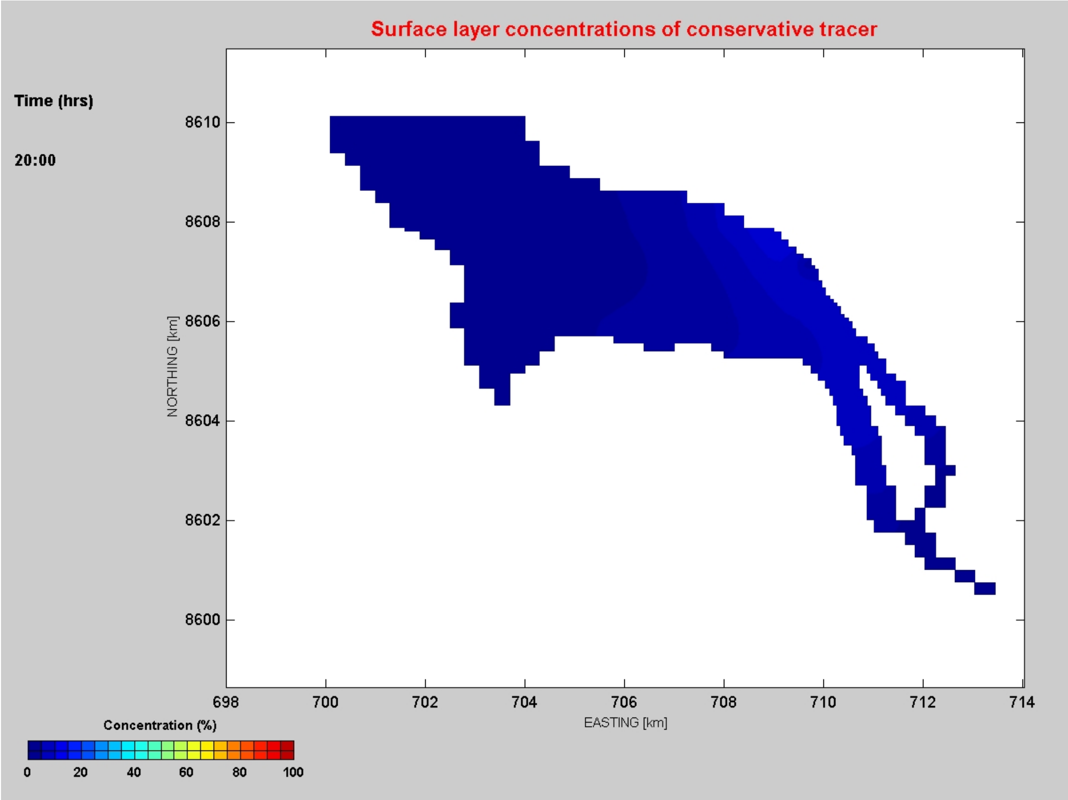

Figure 3.8– Concentrations of conservative tracer after 5 hrs of cease of discharge.

4 References

Backhaus, J. O., 1985. A three-dimensional model for the simulation of shelf-sea dynamics. Deutsche Hydrographische Zeitschrift 38: 165–187.

Backhaus, J., and D. Hainbucher. 1986. A finite difference general circulation model for shelf seas and its application to low frequency variability on the North European Shelf. In: *Three-dimensional models of marine and estuarine dynamics.* eds. Nihoul, J. C. J., and Jamart, B. M.. Elsevier Oceanography Series 45, Elsevier Amsterdam. pp. 221–244.

Backhaus, J., P. B. Crean, and D. K. Lee. 1987. On the application of a three-dimensional numerical model to the waters between Vancouver Island and the main land cost of British Columbia and Washington State. *In*: Heaps, N.M. (ed) *Three dimensional coastal ocean models*, Coastal and Estuarine Sciences Vol. 4, American Geophysical Union, pp. 149–176.

David Williams, 2005. Personnal communications.

Kellogg Brown & Root 2004. PLOOM 3.2: Hydrodynamic modelling of Perth's Wastewater Outlets. Kellogg Brown & Root, May 2004.

Kinhill, 1997a. Perth Long-term Ocean Outlet Monitoring Programme: report on hydrodynamic modelling. Report prepared by Dr K. Zic and C. Gomes on behalf of Kinhill Pty Ltd for the Water Corporation of Western Australia. Perth: Kinhill Pty Ltd.

Kinhill 1997b. Perth Long-term Ocean Outlet Monitoring Programme: Projects M1: Nearfield/farfield modelling. Report prepared by Dr. K. Zic and Mr. C. Gomes on behalf of Kinhill Pty. Ltd. for the Water Corporation of Western Australia. Perth: Kinhill Pty. Ltd.

Kinhill, 1998a. Perth Long-term Ocean Outlet Monitoring Programme: report on hydrodynamic modelling. Report prepared by Dr K. Zic and C. Gomes on behalf of Kinhill Pty Ltd for the Water Corporation of Western Australia. Perth: Kinhill Pty Ltd.

Kinhill, 2000. Hydrodynamic and Ecologhical Studies in Cone Bay, Western Australia. Preliminary Hydodynamic investigations Report by Kinhill Pty Ltd to Maxima Pearling Co Pty Ltd.

Kinhill, 2000. Hydrodynamic and Ecologhical Studies in Cone Bay, Western Australia. Preliminary Hydodynamic investigations Report by Kinhill Pty Ltd to Maxima Pearling Co Pty Ltd.

KBR, 2001. Pearl-farm site selection studies, Kimberley Region, Western Australia. Report by KBR Pty Ltd to Broome Pearls.

KBR, 2001. ‚Preparation of a 'notice of referral', lobster processing facility, Port Denison, Western Australia, Report by KBR Pty Ltd to Kailis Pty Ltd.

Pohlmann, T. 1986. A three dimensional circulation model of the south China Sea. *In*: Nihoul J. C. J. and Jamart B. M. *Three-dimensional models of marine and estuarine dynamics*. Elsevier Oceanography Series 45, Elsevier Amsterdam. pp. 245–268.

Stronach, J. A., J. O. Backhaus, and T. S. Murty. 1993. An update on the numerical simulation of oceanographic processes in the waters between Vancouver Island and the mainland: The GF8 model. *Oceanographic Marine Biology Annual Review* 31: 1–86.

Wilson, D., Padovan A. and Townsend S., The water quality of spring and neap tidal cycles in the middle arm of Darwin harbour during the dry season, Water Monitoring Branch, NRMD, Dept of Infrastructure, Planning and Environment, NT.

APPENDIX A. HYDRODYNAMIC MODEL THEORY

Model description

The key characteristics of the model are as follows (Backhaus, 1985):

- The time-stepping is semi-implicit, allowing for larger time steps than in the commonly used explicit scheme.
- The vertical eddy viscosity depends on both the shear and the Richardson number.
- The vertical momentum equation is simplified by invoking the hydrostatic assumption.
- The employed finite difference scheme is based on the Arakawa C grid (Arakawa and Lamb 1977).

The Cartesian coordinate system for the model is one with the *x*-axis directed eastward, the *y*-axis directed northward, and the *z*-axis positive upward. The zero of the *z*-axis is taken at a horizontal geopotential, approximately at mean sea level. The continuous partial differential equations of the model are as follows:

Mass conservation:

$$\frac{\partial u}{\partial x} + \frac{\partial v}{\partial y} + \frac{\partial w}{\partial z} = 0 \quad \text{(A1.1)}$$

X-directed momentum conservation:

$$\frac{\partial u}{\partial t} - fv + \frac{1}{\rho}\frac{\partial p}{\partial x} + u\frac{\partial u}{\partial x} + v\frac{\partial u}{\partial y} + w\frac{\partial u}{\partial z} = \frac{\partial}{\partial x}(A_H \frac{\partial u}{\partial x}) + \frac{\partial}{\partial y}(A_H \frac{\partial u}{\partial y}) + \frac{\partial}{\partial z}(A_V \frac{\partial u}{\partial z}) \quad \text{(A1.2)}$$

Y-directed momentum conservation:

$$\frac{\partial v}{\partial t} + fu + \frac{1}{\rho}\frac{\partial p}{\partial y} + u\frac{\partial v}{\partial x} + v\frac{\partial v}{\partial y} + w\frac{\partial v}{\partial z} = \frac{\partial}{\partial x}(A_H \frac{\partial v}{\partial x}) + \frac{\partial}{\partial y}(A_H \frac{\partial v}{\partial y}) + \frac{\partial}{\partial z}(A_V \frac{\partial v}{\partial z}) \quad \text{(A1.3)}$$

Conservation of temperature, salinity and/or density:

$$\frac{\partial \theta}{\partial t} + u\frac{\partial \theta}{\partial x} + v\frac{\partial \theta}{\partial y} + w\frac{\partial \theta}{\partial z} = \frac{\partial}{\partial x}(N_H \frac{\partial \theta}{\partial x}) + \frac{\partial}{\partial y}(N_H \frac{\partial \theta}{\partial y}) + \frac{\partial}{\partial z}(N_V \frac{\partial \theta}{\partial z}) \quad \text{(A1.4)}$$

Hydrostatic equation:

$$\frac{\partial p}{\partial z} = -\rho g \quad \text{(A1.5)}$$

with

$$\rho = \rho_o + \sigma_t \quad \text{(A1.6)}$$

In Equations A.1.1 to A.1.6, the dependent variables are defined as follows:

- *u (x, y, z, t)* = velocity component in the *x*-direction
- *v (x, y, z, t)* = velocity component in the *y*-direction

- *w (x, y, z, t)* = velocity component in the *z*-direction
- *f* = Coriolis parameter
- p (x, y, z, t) = pressure
- ρ *(x, y, z, t)* = density
- ρ_o = reference density
- σ_t *(x, y, z, t)* = 1000 (ρ –1.)

  θ = conservative property (temperature, salinity and/or density)
- A_H = horizontal kinematic eddy viscosity
- A_V = vertical kinematic eddy viscosity
- N_H = horizontal eddy diffusivity
- N_V = vertical eddy diffusivity.

In the momentum equations the stress terms are expressed in terms of diffusion coefficients, since this is how these terms are ultimately evaluated in the model. The horizontal eddy coefficient A_H is taken as a constant, whereas the vertical eddy viscosity A_V is assumed to depend on vertical shear and also on the Richardson number in the case of baroclinic flows.

Vertical Mixing (A_V)

The vertical eddy viscosity (A_V) is specified according to Kochergin (1987) where A_V is a function of the velocity gradient and stratification between the layers:

$$A_V = \left(C_L h_L\right)\sqrt{\left(\frac{\partial u}{\partial z}\right)^2 + \left(\frac{\partial v}{\partial z}\right)^2 - \frac{g}{\rho_o}\frac{\partial \rho}{\partial z}} \quad \text{(A1.7)}$$

Here, *u* and *v* are the horizontal velocities, *g* is the gravity, C_L is a constant (= 0.05) and h_L is the thickness of the thermocline. Dividing equation (A.1.7) by $\left(\frac{\partial u}{\partial z}\right)^2 + \left(\frac{\partial v}{\partial z}\right)^2$ gives,

$$A_V = \left(C_L h_L\right)^2 \sqrt{\left(\frac{\partial u}{\partial z}\right)^2 + \left(\frac{\partial v}{\partial z}\right)^2}\sqrt{1 - R_i} \quad \text{(A1.8)}$$

where, R_i is the gradient Richardson number defined by

$$R_i = -\frac{g\frac{\partial \rho}{\partial z}}{\left(\frac{\partial u}{\partial z}\right)^2 + \left(\frac{\partial v}{\partial z}\right)^2} \quad \text{(A1.9)}$$

The vertical diffusivity N_v, for the conservation of salinity and temperature (equation A.1.4) is given by,

$$N_v = A_v\, R_f \big/ R_i \quad \text{(A1.10)}$$

where R_f is the flux Richardson Number defined as,

$$R_f = 0.725\left(R_i + 0.186 - \sqrt{R_i^2 - 0.316 R_i + 0.0346}\right) \text{ (A1.11)}$$

Boundary conditions

The boundary conditions required at the sea surface and at the seabed fall into two categories. The kinematic boundary condition at both surfaces and the bottom stress boundary condition are incorporated directly into the finite difference equations of the model. On the other hand, the wind stress on the sea surface is an external force, and must be parameterised in terms of the applied wind field.

The stress exerted by the seabed on the water column is given by:

$$A_V \frac{\partial u}{\partial z_{bottom}} = F_c u_{bottom} \sqrt{u_{bottom}^2 + v_{bottom}^2} \quad \text{(A1.12)}$$

$$A_V \frac{\partial v}{\partial z_{bottom}} = F_c v_{bottom} \sqrt{u_{bottom}^2 + v_{bottom}^2} \quad \text{(A1.13)}$$

where F_c is the drag coefficient at the seabed, u_{bottom} and v_{bottom} are the velocities in the bottom layer in both the x and y direction respectively.

At the surface of the water, the wind stress is given by:

$$A_V \frac{\partial u}{\partial z_{surface}} = \frac{1}{\rho_{water}} C_D \rho_{air} u_{wind} \sqrt{u_{wind}^2 + v_{wind}^2} \quad \text{(A1.14)}$$

$$A_V \frac{\partial v}{\partial z_{surface}} = \frac{1}{\rho_{water}} C_D \rho_{air} v_{wind} \sqrt{u_{wind}^2 + v_{wind}^2} \quad \text{(A1.15)}$$

where C_D is the drag coefficient at the air/water interface, u_{wind} and v_{wind} are the wind components in the *x* and *y* direction respectively and ρ_{air} is the density of air.

At the land boundaries a non-slip condition has been used.